HIGH-SENSITIVITY FLEXIBLE LIG/GO HUMIDITY SENSORS FOR CONTINUOUS ENVIRONMENTAL MONITORING IN AGRICULTURAL APPLICATIONS

Andrei La Rosa[1,2], Paula Silveira[1,3], Betty Braga Gallo[1,2], Bruno Lopes[1,2], Lucas Gonçalves[1,2], Neftalí Carreño[1,2]

Center for Embedded Devices and Research in Digital Agriculture (CEDRA)[1]; Federal University of Pelotas (UFPEL)[2]; Federal University of Rio Grande do Sul (UFRGS)[3];

A paper from the Proceedings of the

17th International Conference on Precision Agriculture and 11th Brazilian Congress on Precision and Digital Agriculture

13-15 July 2026

Porto Alegre, Brazil

Abstract.

Efficient agricultural production increasingly depends on the continuous monitoring of environmental variables, especially humidity, which directly affects plant physiology, soil behaviour, irrigation management, and the quality of plant materials during storage and transport. In this context, flexible and low-cost sensors can support the development of in situ monitoring systems that are adaptable to different agricultural surfaces and operating conditions. This study presents the development and evaluation of a flexible capacitive humidity sensor based on laser-induced graphene (LIG) and graphene oxide (GO). The sensor was fabricated using direct laser writing on a polyimide substrate to produce interdigitated LIG electrodes, followed by GO deposition as the humidity-sensitive layer. A group of 12 sensors was evaluated in terms of sensitivity, physicochemical behaviour, and electrical response under controlled humidity conditions. Flexibility tests were carried out with 3 sensors, while storage stability was assessed with 6 sensors under ambient laboratory conditions. The electrical response was analysed using a logarithmic regression model. The model described the sensor behaviour well, with coefficients of determination (R^2) usually above 0.97, low residual dispersion, and reduced uncertainty. The angular coefficients (a) were concentrated around 10 %RH/ln(pF), while the intercepts (b) ranged mainly from -35 to -45 %RH, indicating good consistency among the fabricated devices. Only one sample showed discrepant behaviour, with R^2 close to 0.71. The humidity-dependent sensitivity reached an average value of approximately 3.2×10^3 pF/%RH in the 10–90 %RH range.. Mechanical bending tests showed good robustness, with capacitance variations below 2 nF even at a 15 mm bending radius, except under very low humidity conditions. Storage tests performed over 528 h showed no clear loss of performance in the control group. Overall, the results demonstrate that LIG/GO sensors combine high sensitivity, flexibility, repeatability, and short-term stability, supporting their potential integration into future in situ agricultural monitoring systems.

Keywords.

Capacitive humidity sensor, Laser-induced graphene, Linear regression, Durability test.

La Rosa, A., Silveira, P., Gallo, B. B., Lopes, B., Gonçalves, L., & Carreño, N. (2026). High-sensitivity flexible LIG/GO humidity sensors for continuous environmental monitoring in agricultural applications. In Proceedings of the 17th International Conference on Precision Agriculture and 11th Brazilian Congress on Precision and Digital Agriculture (unpaginated, online). Porto Alegre, Brazil: International Society of Precision Agriculture and Brazilian Congress on Precision and Digital Agriculture.

Introduction.

Agribusiness is currently one of the main pillars of the Brazilian economy. In 2024, it represented approximately 22% of the national GDP, equivalent to R$ 2.58 trillion, according to estimates from the Confederation of Agriculture and Livestock of Brazil (CNA, 2024). This strong participation is related to the country's large territorial area, productive diversity, and favourable climatic conditions. However, maintaining efficient agricultural production also requires dealing with growing challenges, such as continuous monitoring of environmental variables, adequate management of inputs, and preservation of product quality during storage and transport. In agricultural systems, plants exposed to water or thermal stress may show complex metabolic changes, including reduced growth rate, lower photosynthetic activity, and increased cellular energy demand (GUPTA; RICO-MEDINA; CANO-DELGADO, 2020; WU et al., 2022).

In this context, advanced materials have become promising alternatives for producing sensors that are more sensitive, flexible, and scalable. In 2014, the laser-induced graphene (LIG) technique expanded this potential by allowing the direct and low-cost production of conductive electrodes on commercial polymers (LIN et al., 2014). Lan et al. (2020) reported a flexible and wearable humidity sensor based on interdigitated LIG electrodes produced by laser direct writing (DLW), with GO deposition to increase sensitivity. The device showed a capacitive response, good mechanical and operational stability, and was applied to real-time monitoring of plant transpiration at the bio-interface. Building on that approach, this paper expands the technical understanding of LIG/GO humidity sensors for agricultural applications by replicating the fabrication route and evaluating humidity response, temperature influence, flexibility, storage stability, and measurement uncertainty.

Methodology.

As described in the introduction, LIG has gained attention as a promising material for sensors because of its high electrical conductivity, porous structure, and scalable fabrication. LIG is formed by the thermal conversion of carbon-rich precursor materials, such as polyimide, when exposed to a high-intensity laser beam. Fig. 1 shows the fabrication route used to produce LIG-based interdigitated electrodes (IDEs) for capacitive humidity sensing.

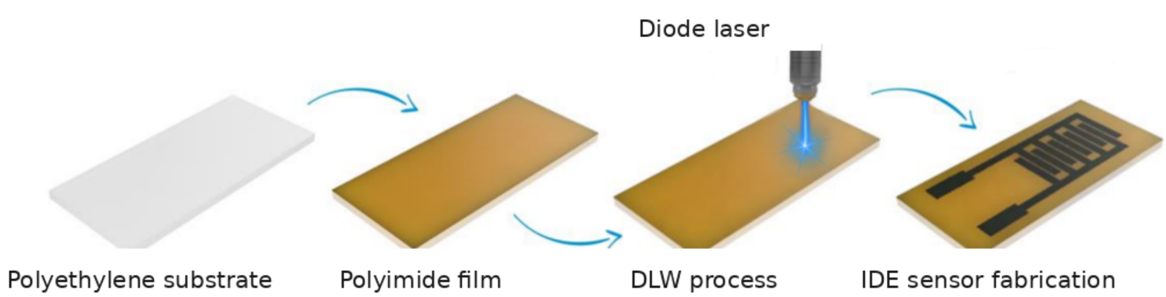

Fig. 1. Fabrication route for LIG-based interdigitated electrodes used in capacitive humidity sensors.

The fabrication of the sensors was performed using DLW on a polyimide substrate, employing a 450 nm diode laser with power adjusted to 9% carbonization of the total 20 W output power. Functionalization was performed by depositing 70 µL of a GO solution (5 mg·mL^{-1} in deionized water) onto the interdigitated electrodes using the drop-casting technique, followed by controlled drying for 12 hours. The study evaluated the sensitivity and physicochemical and electrical characteristics of a group of 12 sensors, as well as flexibility tests conducted on a subset of 3 sensors and storage stability assessments performed on a subset of 6 sensors.

The first experiment evaluated the proof of concept for humidity measurement and the possible influence of temperature. Humidity tests were performed in a climatic chamber (Visomes Plus3)

with controlled temperature and relative humidity. For the humidity response test, the chamber temperature was kept constant at 20 °C. The initial humidity was set to 20 %RH and was increased by 10 %RH every hour until reaching 90 %RH. The capacitance was measured with a Hikari HX 120 digital LCR meter operating at 100 Hz. A calibrated Rotronic HP32 thermo-hygrometer was used as the reference instrument for humidity and temperature. For each humidity level, 30 measurements were recorded.
In addition, the temperature response of the humidity sensor was evaluated. In this test, the chamber humidity was fixed at 50 %RH, while the temperature was increased from 20 °C to 60 °C in steps of 10 °C every 30 min. The same measurement setup and reference instrument described for the humidity test were used. For each temperature level, 30 measurements were recorded.
For the flexibility tests, five D-shaped bending structures were produced by 3D printing with nominal heights of 2.99 ± 0.01 mm, 5.90 ± 0.01 mm, 9.05 ± 0.01 mm, 12.01 ± 0.01 mm, and 15.00 ± 0.01 mm. Each height produced a different bending condition. Each structure included a bending base and a pressure-fit holder to keep the sensor in position, with additional fixation using adhesive tape. Progressive bending tests were performed with three sensors. After each bending step, the sensors returned to the unbent state before the next condition was applied.
The humidity sensors were modelled using a logarithmic calibration equation:

$$RH = a\ ln(C) + b \tag{1}$$

Where: *RH* is the relative humidity (%RH);

a is the angular coefficient;

ln(C) is the logarithm of the capacitance measurement (pF);

b is the linear coefficient.

The input variable C, expressed in pF, was converted to ln(C) before analysis. This transformation linearises the relationship with relative humidity and allows the use of linear regression and ANOVA. The significance of the regression coefficients was tested using Student's t-test to verify whether the estimated coefficients were statistically different from zero. In sensor calibration, the angular coefficient represents the sensitivity of the sensor response to the reference quantity; therefore, its statistical significance indicates evidence of a relationship between the analysed variables (MONTGOMERY; PECK; VINING, 2012; PENNSTATE, 2025a). The global significance of the regression model was also assessed using the F-test. The Shapiro-Wilk, Jarque-Bera, and Anderson-Darling tests were used to evaluate the normality of residuals. Homoscedasticity was assessed using the Breusch-Pagan test, which verifies whether the residual variance remains constant. The independence of residuals was evaluated using the Durbin-Watson statistic. The computational analysis was performed using functions from the SciPy library (SciPy Developers, 2026a,b,c). Finally, a complete uncertainty analysis was performed, including contributions from standard deviation, hysteresis, flexibility, measurement instrument, and climatic chamber stability, leading to the expanded uncertainty (GUM, 2008; INMETRO, 2020).
For the storage stability test, 6 sensors were monitored as the control group. The complete test lasted 528 h, from 3 November 2025 to 25 November 2025, under ambient laboratory conditions.

Results.

The experimental evaluation first focused on verifying whether the fabricated LIG/GO IDE sensor could detect controlled humidity variations and whether its response was affected by temperature changes under fixed humidity conditions. Fig. 2a shows one fabricated sensor and the proof-of-concept results obtained during humidity and temperature tests. The comparison with the commercial Rotronic HP32 thermo-hygrometer indicates that the IDE sensor follows the humidity increase observed by the reference instrument. In the humidity test, relative humidity is represented on the right axis, while the capacitance response of the developed sensor is represented on the left axis using a logarithmic scale (Fig. 2b). Fig. 2c also presents the capacitance response under temperature variation, with chamber humidity fixed at 50 %RH. The sensor response increased with temperature, which indicates that temperature may affect capacitance readings, especially under low-humidity conditions. For the temperature range used during the humidity test, this temperature effect represented approximately 10% of the measured capacitance value.

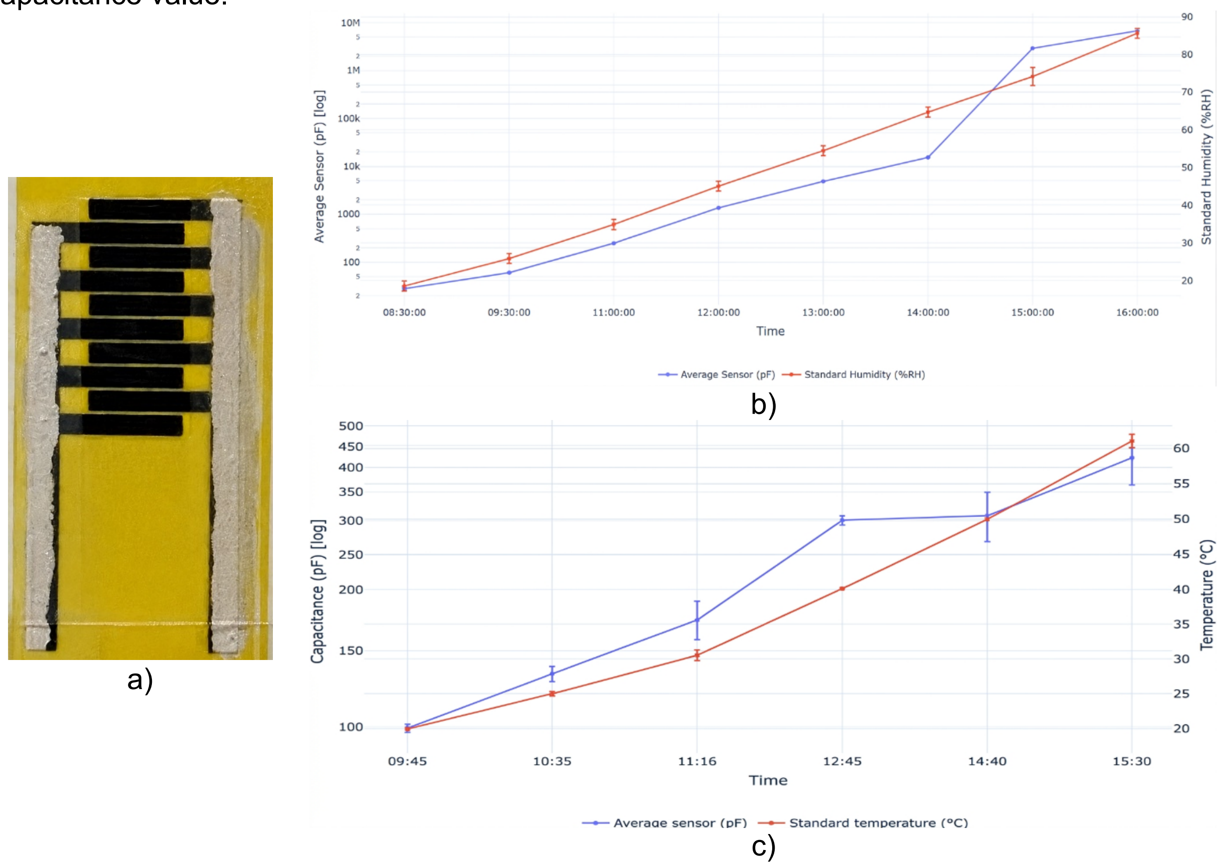

Fig. 2. Fabricated LIG/GO sensor and proof-of-concept response under controlled humidity and temperature tests.

Capacitance increased exponentially with relative humidity, which is expected for capacitive sensors based on hydrophilic dielectric materials. This behaviour supports the suitability of the adopted LIG/GO sensing approach. This response can be explained by the physicochemical interaction between graphene oxide and water molecules. In the GO-modified IDE sensor, the humidity response is related to adsorption and desorption of water molecules on the surface and between GO layers. According to Zhu et al. (2020), GO is hydrophilic because it contains oxygenated functional groups, such as hydroxyl, epoxy, and carboxyl groups. These groups act as active sites for hydrogen bonding with H_2O molecules, changing the dielectric permittivity of the film and increasing capacitance.

At low relative humidity, water adsorption occurs mainly through stronger hydrogen bonds, which restrict molecular mobility and produce small capacitance changes. As humidity increases, adsorbed water molecules become more mobile, and partial ionisation under the electric field between the IDEs may occur. In this condition, hydronium ions (H_3O+) can contribute to electrical conduction and increase the effective dielectric constant. At high humidity, water may penetrate the interlamellar space of GO, creating more continuous ionic conduction paths and leading to the sharp capacitance increase observed experimentally. Therefore, the exponential response of the LIG/GO sensor reflects the gradual transition from physical adsorption to ionic conduction mechanisms, in agreement with the behaviour reported by Lan et al. (2020) and Zhu et al. (2020) for high-sensitivity GO-based humidity sensors.

Table 1 presents the repeatability and reproducibility percentages for each relative humidity level. The humidity sensors showed high repeatability, with the variance associated with repeated measurements remaining very low, usually below 0.1% and reaching about 1.7% only at 89.6%RH. However, reproducibility accounted for more than 98% of the total variance in all conditions, indicating significant differences between sensors. Therefore, although each sensor provides consistent measurements, the devices should not be considered interchangeable without individual calibration or sensor-specific correction.

Table 1. Repeatability and reproducibility contribution by relative humidity level.

Umidade (%RH)	Repet. (%)	Repro. (%)	repetibilidade	reprodutibilidade
18.70	0.100844	99.899156	☑	☒
28.32	0.089285	99.910715	☑	☒
38.38	0.016601	99.983399	☑	☒
48.29	0.033399	99.966601	☑	☒
57.30	0.007953	99.992047	☑	☒
67.95	0.010190	99.989810	☑	☒
78.70	0.005791	99.994209	☑	☒
89.58	1.734972	98.265028	☑	☒

The regression analysis provided a detailed view of the calibration behaviour of the evaluated humidity sensors, as summarised in Table 2. In general, the logarithmic regression model showed a good fit to the experimental data, with R^2 values above 0.99 for most sensors, indicating a strong relationship between capacitance and relative humidity. The angular coefficients (a) were mainly concentrated around 10 %RH/ln(pF), while the intercepts (b) varied between approximately −24 and −45 %RH, showing a similar response trend among most devices. Sensor 16 was the only discrepant sample, with a lower R^2 value of 0.7147 and regression coefficients substantially different from the others, suggesting an atypical electrical response or fabrication-related variation.

The t-test and global model significance results were positive for all sensors, confirming that the regression coefficients and the proposed model are statistically significant. However, the residual diagnostic tests indicated limitations in the statistical assumptions of the model, since normality, homoscedasticity, and residual independence were not fully satisfied. Therefore, although the model is useful to describe the calibration behaviour and compare the sensors, the residual analysis suggests that additional effects, such as sensor-to-sensor variability, hysteresis, or environmental fluctuations, may influence the response. These results reinforce the need for individual calibration of each sensor before practical application.

Table 2. Regression coefficients and residual diagnostic tests for the evaluated sensors.

N° of sensor	a	b	R^2	t-test	Model significance	Norm.	Homosc.	Residual ind.
15	10.3378	-38.0553	0.9959	☑	☑	☒	☒	☒
16	21.8624	103.7506	0.7147	☑	☑	☒	☒	☒
22	10.8873	-45.0844	0.9942	☑	☑	☒	☒	☒
26	10.2932	-37.1189	0.9959	☑	☑	☒	☒	☒
28	10.1470	-36.8414	0.9981	☑	☑	☒	☒	☒
30	10.1691	-33.8831	0.9987	☑	☑	☒	☒	☒
34	10.5053	-40.0207	0.9944	☑	☑	☒	☒	☒
36	10.8147	-40.3494	0.9983	☑	☑	☒	☒	☒
41	10.2351	-35.4165	0.9969	☑	☑	☒	☒	☒
42	9.63619	-24.4514	0.9996	☑	☑	☒	☒	☒
43	10.6980	-29.9314	0.9995	☑	☑	☒	☒	☒

45	10.5825	-36.5188	0.9996	☑	☑	☒	☒	☒

The uncertainty behaviour of sensor 15 was evaluated by considering the main contributions involved in the measurement process, as shown in Fig. 3. The plotted components include the uncertainty related to standard deviation (sd), chamber stability (stab), inherited uncertainty from the reference instrument (ref), sensor flexibility (flex), hysteresis (hist), instrument resolution (res), and instrument precision (prec). Overall, the results show that the measurement system had better repeatability than global metrological capability. In most of the humidity range, the combined standard uncertainty remained around 1 to 2 %RH, resulting in expanded uncertainties between 3 and 8 %RH.

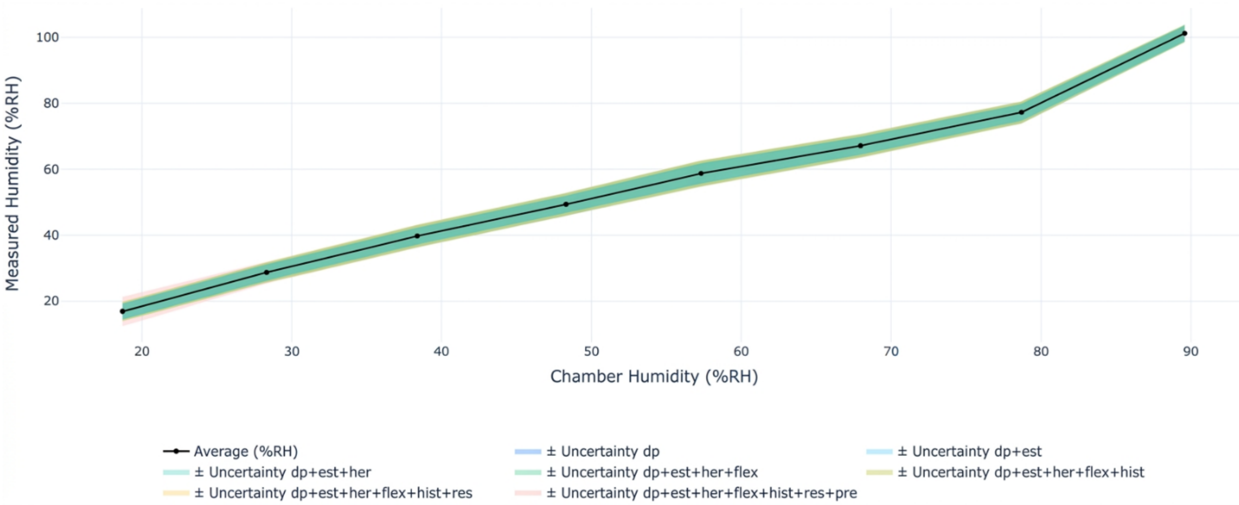

Fig. 3. Expanded uncertainty analysis for sensor 15 over the tested relative humidity range

The flexibility tests showed that bending had a limited influence on the capacitive response of the humidity sensors. Under the evaluated bending conditions, the capacitance variation did not exceed 2 nF, indicating that the flexible LIG/GO structure preserved its sensing behaviour after mechanical deformation. This result supports the use of the humidity sensor in flexible monitoring platforms, although further tests under repeated bending cycles are still required for field applications.

The storage stability of the devices was assessed by monitoring six control sensors for approximately 528 h under ambient laboratory conditions, as shown in Fig. 4. For all sensors, most measurements remained within the expected capacitance range, on the order of tens of nF. This indicates that the devices preserved their characteristic electrical response during the test and remained consistent with the environmental conditions to which they were exposed, without clear evidence of degradation or loss of functionality.

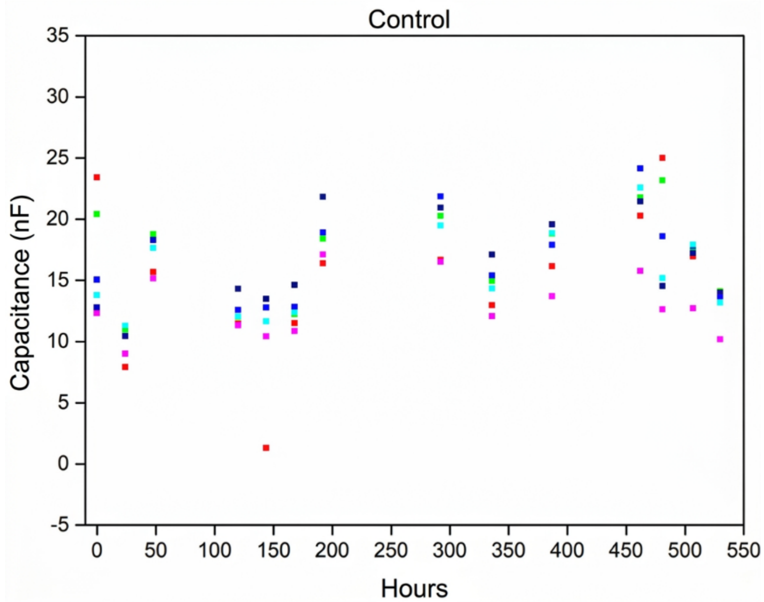

Fig. 4. Storage stability of six LIG/GO control sensors during 528 h under ambient laboratory conditions.

Conclusions.

This study demonstrated the fabrication and evaluation of flexible capacitive humidity sensors based on laser-induced graphene and graphene oxide for agricultural monitoring applications. The DLW fabrication process on polyimide, followed by GO functionalization, produced interdigitated electrodes with a clear humidity-dependent capacitive response. The logarithmic calibration model described the relationship between capacitance and relative humidity well for most sensors, with high R^2 values and statistically significant models. However, the residual tests showed that the assumptions of normality, homoscedasticity, and independence were not fully satisfied, indicating that additional effects may influence the sensor response.

The sensors showed high repeatability under the same measurement conditions, but low reproducibility between devices, confirming that individual calibration or sensor-specific correction is necessary. Mechanical tests showed only a small influence of bending on the humidity response, with capacitance variations not exceeding 2 nF, while the 528 h storage test showed no clear degradation in the control group. The uncertainty analysis also indicated a limited influence of the evaluated parameters under the tested conditions.

Overall, the results confirm the potential of LIG/GO humidity sensors as flexible, sensitive, and low-cost devices for in situ agricultural monitoring. Future work should focus on improving sensor-to-sensor reproducibility, reducing temperature influence, validating the sensors under real field conditions, and integrating calibration strategies into embedded monitoring platforms.

Acknowledgements.

This work has been partially funded by the project AgroHeath supported by the Center for Embedded Devices and Research in Digital Agriculture (CEDRA) of SENAI-RS, with financial resources from the PPI IoT/Manufatura 4.0 / PPI HardwareBR of the MCTI, grant number 056/2023, signed with EMBRAPII.

References.

CNA, C. d. A. e. P. d. B. ***Relatorio do PIB do Agronegocio Brasileiro 2024****. https: //www.cnabrasil.org.br.*

GUM, I. ***Evaluation of measurement data – Guide to the expression of uncertainty in measurement****. [S.l.]: JCGM, 2008. GUM 1995 with minor corrections. (JCGM*

100:2008).
GUPTA, A.; RICO-MEDINA, A.; CANO-DELGADO, A. I. The physiology of plant responses to drought. ***Science****, [S.l.], v.368, n.6488, p.266–269, 2020.*
LAN, L. et al. One-step and large-scale fabrication of flexible and wearable humidity sensor based on laser-induced graphene for real-time tracking of plant transpiration at bio-interface. ***Biosensors and Bioelectronics****, [S.l.], v.165, p.112360, 2020.*
LIN, J. et al. Laser-induced porous graphene films from commercial polymers. ***Nature Communications****, [S.l.], v.5, p.5714, 2014.*
MONTGOMERY, D. C.; PECK, E. A.; VINING, G. G. ***Introduction to Linear Regression Analysis****. 5.ed. Hoboken, NJ: John Wiley & Sons, 2012.*
PENNSTATE. ***The General Linear F-Test****. STAT 501: Regression Methods. Disponivel em: <https://online.stat.psu.edu/stat501/lesson/6/6.2>. Acesso em: 2026-05-02.*
SciPy Developers. ***scipy.stats.shapiro****. SciPy documentation. Disponivel em: <https://docs.scipy.org/doc/scipy/reference/generated/scipy.stats.shapiro.html>. Acesso em: 2026-05-02.*
SciPy Developers. ***scipy.stats.jarque_bera****. SciPy documentation. Disponivel em: <https://docs.scipy.org/doc/scipy/reference/generated/scipy.stats.jarquebera.html > .Acessoem : 2026 − 05 − 02.*
SciPy Developers. ***scipy.stats.anderson****. SciPy documentation. Disponivel em: <https://docs.scipy.org/doc/scipy/reference/generated/scipy.stats.anderson.html>. Acesso em: 2026-05-02.*
WU, J. et al. Physiology of plant responses to water stress and related genes: A review. ***Forests****, [S.l.], v.13, n.2, p.324, 2022.*
ZHU, C. et al. Graphene oxide humidity sensor with laser-induced graphene porous electrodes. ***Sensors and Actuators B: Chemical****, [S.l.], v.325, p.128790, 2020.*